RSC Advances

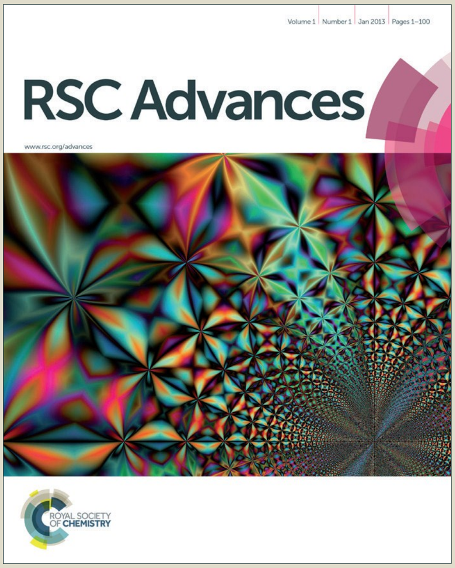

ROYAL SOCIETY OF CHEMISTRY

www.rsc.org/advances

Toward Unsaturated Stannylenes Y_2Z=Sn: and Related Compounds with Triplet Electronic Ground States

Ashwini Bundhun[1], Mohammad R. Momeni[2], Farnaz A. Shakib[2], Ponnadurai Ramasami[1]*,
Peter P. Gaspar[3]*, and Henry F. Schaefer III[4]*
[1]Computational Chemistry Group, Department of Chemistry, University of Mauritius, Réduit, Mauritius
[2]Department of Chemistry, Shahr_e Qods Branch, Islamic Azad University, Tehran 37515-374, Iran
[3]Department of Chemistry, Washington University, Saint Louis, Missouri 63130, USA
[4]Center for Computational Quantum Chemistry, University of Georgia, Athens, Georgia 30602, USA

Abstract: A new series of unsaturated stannylenes is studied computationally. The singlet and triplet states of acyclic and cyclic stannylenes are fully optimized using the B3LYP, BHLYP, OPBE, and M06 functionals. The basis sets used are of double-ξ plus polarization quality with additional s- and p-type diffuse functions denoted DZP++. All cyclic and most acyclic stannylenes have been found to have triplet ground states. The most favored triplet state is that for the NHC (NMeCHCHNMe)Sn=Sn: system, where the triplet state lies ~20 kcal mol^{-1} below the singlet. The saturated cyclic systems are expected to be easier to synthesize, but the unsaturated cyclic counterparts have larger singlet-triplet splittings. A preparative outline based on retro-synthetic routes is briefly described.

*Corresponding authors. E-mail: ramchemi@intnet.mu (PR), gaspar@wustl.edu (PPG) and ccq@uga.edu (HFS)

1. Introduction

Carbenes, neutral molecules R_2C: containing divalent carbon atoms, have fascinated chemists for more than a half century because they exist in two accessible spin states, each with its own distinctive chemistry [1-3]. Their tin analogs, stannylenes, have been generated in solution only with singlet ground states, and, until 2009, when the preparation of 1-stannacyclopent-3-enes provided convenient precursors for a variety of stannylenes [4], most of these were produced with bulky substituents which discourage bimolecular reactions by steric shielding [5,6].

Reactions of sterically hindered stannylenes are comparatively slow and oligomerization is very rapid. Now stannylenes containing smaller substituents such as Me and Ph can be generated both thermally and photochemically, and the chemistry of ground state singlet stannylenes can now be more thoroughly explored, employing stannylenes whose intermolecular reactions are competitive with oligormerization [4].

The motivation to study stannylenes R_2Sn:, is that the lowest singlet electronic states of the analogous carbenes, silylenes, and germylenes undergo synthetically useful stereospecific addition and insertion reactions with concerted formation of two bonds [3,5]. The chemistry of singlet stannylenes found by Neumann [6] and Lappert [7] also promises synthetic utilization. Calculations on the addition of Me_2Sn: to butadiene predict a concerted asynchronous addition, and predicted activation parameters for the retro-addition are in decent agreement with the experimental results [8]. For the triplet stannylenes studied here, it is most desirable to have a sufficiently large singlet-triplet gap so that the reactions observed will be exclusively those of the triplet ground state.

Unsaturated heavier group 14 carbene analogs have already received some attention. Singlet states of unsaturated silylenes and germylenes have been studied. Worthington and Cramer [9] performed DFT computations on the effects of substituents on the singlet-triplet energy gaps of unsaturated carbenes, the XYC=C:. Irikura, Goddard, and Beauchamp [10] suggested that hyperconjugative electron-donation from the singly occupied carbene p-orbital to the C−F σ* orbital plays a major role in lowering the energy of the triplet states. A lesser stabilizing substituent effect was proposed to be inductive electron-withdrawal from the n-orbital at the carbene center.

In this work, double-bonded Y_2Z=Sn: (Z = C, Si, Ge, and Sn; Y = H, F, $NMeCH_2$– and NMeCH–) species are investigated, with the prime objective to reliably predict their singlet-triplet gaps. Many of these species were expected to contain stannylene centers sufficiently sterically unshielded to permit bimolecular reactions and to possess triplet ground states. It is hoped that density functional theory computations employing several functionals will provide useful information about their electronic properties that will facilitate their experimental characterization. Hopefully, exploration of the chemistry of triplet stannylenes should be possible for the first time. Interpretation of the computations presented should lead to answers for questions regarding computations on these novel species of vinylidenes. Specifically, the character of the multiple bond between the tin and Z atoms (Z = C, Si, Ge, and Sn) and the effects of substituents Y [11] will be explored.

2. Theoretical Methods

All geometries were fully optimized with the Gaussian 09 Program [12], using four functionals, BHLYP, B3LYP, OPBE and M06 [13]. BHLYP is an HF/DFT hybrid method employing the Becke (B) [14] half and half exchange functional (H) [15] and the Lee, Yang, and Parr (LYP) [16] non-local correlation functional. The ubiquitous B3LYP method combines Becke's three-parameter exchange functional (B3) with the LYP correlation functional. In all cases, an extended integration grid (199974) was used, with very tight convergence criteria applied to all computations. Harmonic vibrational frequencies were evaluated analytically to characterize all stationary points as minima.

Double-ζ basis sets with polarization and diffuse functions, denoted as DZP++, were used for all atoms, except that the valence basis set used for tin incorporates the fully-relativistic Stuttgart-Dresden small-core effective core potential [17]. The double-ζ basis sets were constructed by augmenting the Huzinaga–Dunning–Hay [18-20] sets of contracted Gaussian functions with one set of p polarization functions for each H atom and one set of d polarization functions for each heavy atom, respectively [$\alpha_p(H) = 0.75$, $\alpha_d(C) = 0.75$, $\alpha_d(N) = 0.80$, $\alpha_d(F) = 1.0$, $\alpha_d(Si) = 0.5$]. The above basis sets were further augmented with diffuse functions, where each atom received one additional s-type and one additional set of p-type functions. Each H atom basis set is augmented with one diffuse s-function. The diffuse functions were determined in an even-tempered fashion following the prescription of Lee [21],

$$\alpha_{\text{diffuse}} = \frac{1}{2}\left(\frac{\alpha_1}{\alpha_2} + \frac{\alpha_2}{\alpha_3}\right)\alpha_1$$

where α_1, α_2 and α_3 are the three smallest Gaussian orbital exponents of the s- or p- type primitive functions of a given atom ($\alpha_1 < \alpha_2 < \alpha_3$). Thus $\alpha_s(H) = 0.04415$, $\alpha_s(C) = 0.04302$,

$\alpha_p(C) = 0.03629$, $\alpha_s(N) = 0.06029$, $\alpha_p(N) = 0.05148$, $\alpha_s(F) = 0.1049$, $\alpha_p(F) = 0.0826$, $\alpha_s(Si) = 0.02729$, $\alpha_p(Si) = 0.025$.

The DZP++ basis set for germanium was comprised of the Schafer-Horn-Ahlrichs double-ζ spd set plus a set of five pure d-type polarization functions with $\alpha_d(Ge) = 0.246$, and augmented by a set of sp diffuse functions with $\alpha_s(Ge) = 0.024434$ and $\alpha_p(Ge) = 0.023059$ [22]. The overall contraction scheme for the all-electron basis sets is: H(5s1p/3s1p), C(10s6p1d/5s3p1d), F(10s6p1d/5s3p1d), Si(13s9p1d/7s5p1d), N(10s6p1d/5s3p1d), and Ge(15s12p6d/9s7p3d). Each (adiabatic) singlet-triplet splitting is predicted as the energy difference between the lowest singlet state and its lowest triplet state:

$$\Delta E_{S\text{-}T} = E(\text{optimized triplet}) - E(\text{optimized singlet}).$$

3. Results and Discussion

A. Geometries

The equilibrium geometries for the $^1A_1$ and $^3A_2$ states of $H_2Z{=}Sn$: and $F_2Z{=}Sn$: (Z = C, Si, Ge, and Sn), are reported in **Figures 1–4**. In **Figures 5–8** are the predicted equilibrium geometries for the ^1A and ^3A states of $(NMeCH_2CH_2NMe)Z{=}Sn$: and (NMeCHCHNMe)Z=Sn:. The internal coordinates, theoretical harmonic vibrational frequencies (cm^{-1}), and energies (hartrees) at the BHLYP functional, are available as Supporting Information (SI). There are large differences in the Z=Sn bond lengths along the series of $^1A_1$ singlet states $Y_2Z{=}Sn$: (Y = H, F; Z = C, Si, Ge, and Sn) and their corresponding $^3A_2$ triplet states are presented in **Table 1**.

B. Natural Lewis Structures

Natural bond orbitals (NBO) [23] are computed to search for Lewis structures, representing non-bonding and bonding electron pairs. These may be termed as Natural Lewis Structures, explaining hybridizations and polarization coefficients for each NBO [24].

The Y_2Z: subsystem of the $Y_2Z{=}Sn$: (Z = C, Si, Ge, and Sn) molecules can exist in two low-lying electronic states: $^1A_1$ and $^3B_1$, while the Sn atom itself exhibits a triplet ground state as depicted in **Scheme 1**. Hence, the final electronic state of the stannylene molecule depends on the distribution of the nonbonding electrons in the σ and π orbitals of the Y_2Z: moiety. In the singlet electronic state of the $Y_2Z{=}Sn$: molecule, one of the two nonbonding electrons of the Y_2C: moiety occupies the hybrid σ orbital, which is partly localized on the carbene carbon. The other nonbonding electron occupies the carbene 2pπ atomic orbital, and these electrons have parallel spins, hence $^3A_2$ symmetry. In the corresponding triplet electronic state there are two nonbonding electrons occupying the hybridized σ orbital, which is incompletely localized on the carbene carbon atom, thus a $^1A_1$ state can be designated for the Y_2C: moiety. Since the σ orbital is a hybrid with a contribution from the carbon 2s atomic orbital, this σ orbital is lower in energy than the 2pπ orbital. The π orbital involves a carbon 2p atomic orbital, forming a partially occupied π orbital between the singlet $^1A_1$ Y_2C: carbene moiety and the triplet Sn atom. It is expected that the $^3A_2$ electronic state of the $Y_2Z{=}Sn$: molecules, with a $\sigma^2\pi^0$ configuration in the H_2Z: moiety in the $^1A_1$ singlet $\sigma^2\pi^2$ electronic state of $H_2Z{=}Sn$:, can be favored relative to the $^3B_1{-}\sigma^1\pi^1$ configuration of the H_2Z: moiety by substituents lowering the energy of the pπ atomic orbital and raising the energy of the σ molecular orbital of the H_2Z: moiety. If the Y_2Z: subsystem presents a $^3B_1{-}\sigma^1p^1$ configuration in the $^1A_1$ singlet state of $Y_2Z{=}Sn$:, a lower Coulombic repulsion exists between the nonbonding electrons of the H_2Z: moiety. This allows a triplet $^3A_2$ ground state of Y_2Z=Sn: with $^1A_1$–σ^2p^0 configuration at its Y_2Z: moiety to be stabilized selectively by substituents such as fluorine or a five-membered ring system containing nitrogen lone pair electrons which partially fill the p-orbital, encouraging the shift of an electron from π to p.

As seen in **Table 2**, the singlet ground states of the unsubstituted H_2Z=Sn: (Z = C, Si, Ge, and Sn) are predicted to be energetically preferred to their corresponding triplet states except for H_2Sn=Sn: at BHLYP. The trends in the predicted decreasing energy gaps follow the standard Pauling electronegativities [25] (χ_F = 3.98; χ_C = 2.55, χ_H = 2.20, χ_{Ge} = 2.01, χ_{Sn} = 1.96, and χ_{Si} = 1.90) fairly regularly with the carbon substituent standing apart in predicting the largest singlet-triplet gaps, compared to its analogs in the series studied. The predicted $\Delta E_{S\text{-}T}$ values (kcal mol^{-1}) for H_2C=Sn: are 20.9 (B3LYP), 15.3 (BHLYP), 21.3 (OPBE), and 24.0 (M06), while the Si, Ge, and Sn analogues result in decreases in the $\Delta E_{S\text{-}T}$ (kcal mol^{-1}) to 5.4 (H_2Si=Sn:), 5.2 (H_2Ge=Sn:), and 1.1 (H_2Sn=Sn:) with the B3LYP functional. Similar decreases are predicted with the OPBE functional, while computations with the BHLYP functional predict a triplet ground state for H_2Sn=Sn:.

In order to verify the energies and structures of the $^1A_1$ singlet ground state H2C=Sn: and its corresponding $^3A_2$ triplet state, CCSD(T) computations were performed. The predicted singlet triplet gap is predicted to be 23.8 kcal mol^{-1}, which is very close to the M06 result. The BHLYP functional provides the best agreement of the predicted structures with experimental geometrical parameters. The same functional is found to be the most reliable in predicting structural parameters and electron affinities of germylenes [26]. These may be correlated with the fact that the BHLYP functional incorporates the largest fraction of the Hartree-Fock method [15].

C. Design of Unsaturated Stannylenes

Despite the careful analysis by Worthington and Cramer [9], the nature of the stabilization of the triplet states of unsaturated carbenes remains incompletely understood. Therefore, the goals of our present computations include contributions to that understanding, as well as to the question of unsaturated stannylenes with triplet ground states. Such desirable structures should be sufficiently sterically unhindered at their two-coordinate tin atoms to allow the exploration of the chemistry of the neutral triplet stannylenes.

The theoretical description of Momeni and Shakib [27] of triplet silylenes related to $H_2Si=Si:$ provided some of the motivation for the present exploration of novel unsaturated stannylenes. The substituent effect favoring the triplet state was attributed to the donation of lone pair electrons from Y substituents on $Y_2Si=Si:$ to the half-filled π molecular orbital. Stabilization of the triplet ground states was also credited to the acceptor properties of the β-substituent-silicon antibonding orbitals. The fusion of an Arduengo carbene or silylene onto the unsaturated silylene was suggested by Momeni and Shakib [27] to reduce the rate of silylene loss by rearrangements and to increase the size of the energy gap favoring ground triplet states. Our computations describe the effects of changing the Y-substituent of the $Y_2Z=Sn:$ (Z = C, Si, Ge, and Sn) triplet electronic structures. The relative changes in the geometrical parameters and the predicted singlet-triplet gaps obtained with the different functionals used are found to be reasonably consistent. The BHLYP values are used in discussions within this paper, since this functional appears better than the other functionals employed in the prediction of geometries, harmonic vibrational frequencies, and singlet-triplet splittings [28], for related molecules.

D. Substitution in Stannylenes

The triplet state unsaturated stannylenes arise in a simple picture from the excitation of an electron from the Z=Sn π orbital to the empty 5p orbital component at the Sn atom of the singlet Y_2Z=Sn:. Due to the presence of heavier Group 14 elements as α-substituents, there is a lower tendency for the tin atom to form hybrids of the 5s and 5p orbitals on the stannylene centre. Because of this low tendency for hybridization, the expected singlet-triplet energy gaps between the Sn 5p vacant orbitals and the occupied orbitals are expected to be larger compared to the predicted results for silylenes and carbenes [27]. Synthetic realization of these predictions would allow to the experimental study of triplet stannylenes. Substitutions of the hydrogen atoms by atoms or groups of greater electronegativity are predicted to enhance the double-bond lengths of these stannylenes along with changes in the $\Delta E_{S\text{-}T}$.

The replacement of the carbon substituent by silicon, germanium, and tin atoms, which are more electropositive than carbon, affects the bonding characteristics of the ground state triplet structures as shown in **Table 1**, the predicted Z=Sn bond lengths for the triplet state structures calculated with the BHLYP functional are comparable to the typical C-Sn, Si-Sn, Ge-Sn, and Sn=Sn single bonds of 2.19 Å, 2.60 Å, 2.64 Å, and 2.96 Å, respectively.

One of the two π NBOs for the H_2Si=Sn: system includes the overlapping of the Sn p_x orbital with a hybrid $pd^{0.5}$ orbital of the adjacent H_2Si: substituent [27]. The d orbitals on Sn do not participate significantly in this NBO and instead serve as polarization functions, consistent with results for the H_2Si-Si: molecule [27]. Therefore, this NBO is primarily an Sn 5p orbital which is partly polarized towards the adjacent substituent; hence an asymmetric π bond is formed. The replacement of the carbon atom with heavier group 14 atoms may decrease the singlet-triplet splitting values by a significant margin because their lower electronegativity eases promotion of an electron from a π-orbital [27].

E. Fluorine Substitution

In the difluoro substituted stannylenes, $F_2Y{=}Sn$: (Y = C, Si, Ge, and Sn), the F−Y σ molecular orbital of the F_2Y: moiety contains contributions from the two fluorine atoms. With respect to the standard Pauling electronegativities [25], the greater electronegativity of fluorine $\chi_F = 3.98$ compared to hydrogen $\chi_H = 2.20$ provides stabilization to the σ molecular orbital of the F_2Z: moiety relative to the σ molecular orbital of H_2Z:. The p−π atomic orbital on the Z centre of the Y_2Z: moiety in the lowest singlet state of $Y_2Z{=}Sn$: is destabilized by the delocalisation of a pair of fluorine lone-pair electrons. The pair of electrons that is delocalised into the p−π atomic orbital comes from the in-phase combination of the 2p−π lone pair atomic orbitals on the fluorine atoms. The decrease in the F–Z–F bond angle compared to the predicted H–Z–H bond angles at the Y_2Z centre is a result of an increase in the 2s character of the Z–F σ molecular orbital, which is thus stabilized compared to the σ molecular orbital of ZH_2. The geometries of the lowest lying triplet states of $Y_2C{=}Sn$: (Y = H and F) incorporate the lowest lying singlet states of the H_2C: or F_2C: moiety and should be similar. However, the donation of electrons from the fluorine lone pairs into the empty 2pπ orbital on the carbene centre raises the energy of the LUMO of the $\sigma^2\pi^0$ singlet state of the F_2C:. Hence, the triplet ground state of $F_2C{=}Sn$: displays a longer C=Sn bond. In replacing the carbon atom with Si, Ge, or Sn, the triplet states are found to be the ground states. The singlet-triplet gaps of $F_2Y{=}Sn$: (Y = C, Si, Ge, and Sn) decrease with a decrease in the

Pauling electronegativities. The effect of the fluoro substituents reduces the energy of the triplet state structures compared to the unsubstituted H_2Z=Sn: (Z = C, Si, Ge, and Sn) molecules. The singlet-triplet splitting of F_2C=Sn: is significantly decreased compared to H_2C=Sn:, with the computed values (kcal mol^{-1}) being 2.9 (B3LYP), 1.3 (OPBE), and 8.1 (M06), and at the BHLYP functional the triplet state is found to be lower in energy than its singlet state by –1.4 kcal mol^{-1}. The computed singlet-triplet splitting values with the BHLYP functional for the F_2Z=Sn: (Z = C, Si, Ge, and Sn) are –1.4, –8.2, –8.4, and –11.9 kcal mol^{-1}, respectively.

F. Analogues of N-Heterocyclic Carbenes

Turning to the development of experimentally more viable structures, the cyclization of nitrogen-containing five-membered structures should reduce the probability for any rearrangement of unsaturated stannylenes Z_2Y=Sn:. For this reason we selected the (NMeCHCHNMe) subsystem to favour the triplet systems [27] and to study the effects of σ-donating substituents on the relative energies of the cyclic triplet ground state systems. In order to achieve a change in the relative energies of the N-heterocyclic carbenes the σ molecular orbital at the carbene centre can be raised. The destabilization of this molecular orbital can be achieved by using substituents at the carbene centre which contain lone pairs of electrons. The properties of the cyclic structures engender ring strain due to the presence of the nitrogen atoms. The nitrogen lone pairs have a large effect on reducing the energy differences between the $^1A_1$–$\sigma^2\pi^0$ and $^3B_1$–$\sigma^1\pi^1$ configurations of the carbene centre.

The computed C–N, Si–N, Ge–N, and Sn–N bond lengths (BHLYP) for the saturated cyclic singlet state structures are 1.364 Å, 1.708 Å, 1.825 Å, and 2.028 Å. For the low-lying triplet states the predicted bond lengths are 1.341 Å, 1.702 Å, 1.815 Å, and 2.019 Å, respectively. The C–N bond length for the corresponding triplet unsaturated cyclic structure is predicted to be shorter than that for the singlet while the Si–N, Ge–N, and Sn–N bond lengths are predicted to be longer. However, there are only modest differences in the N–Z–N bond angles in the saturated and unsaturated structures, between the singlet and triplet states (0.1° – 1.7°). The differences in the predicted bond lengths result from the lower ability of the nitrogen atoms in the unsaturated rings to donate electron density to the Z centre. A larger increase in $\Delta E_{S\text{-}T}$ favoring the triplet state was found for the unsaturated five-membered rings (NMeCHCHNMe)Z=Sn: (Z = C, Si, Ge, and Sn).

4. Summary

The work reported here adds understanding of the nature of the energetics of triplet states of unsaturated stannylenes. Another goal of these computations was the design of unsaturated stannylenes with triplet ground states. The research reported here suggests that unsaturated triplet stannylenes $Y_2Sn{=}Sn$: are favored by donation of electron density from a :Y lone pair to a partially occupied 5p-orbital on Sn. This analysis is consistent with the explanation by Momeni and Shakib [27] of the effects of electronegative substituents on triplet unsaturated silylenes, $Y_2Si{=}Si$:. **Table 2** reports the Z=Sn bond lengths and stretching vibrational modes of several unsaturated stannylenes predicted to possess triplet ground states, and their predicted structures are shown in **Figures 1-8**. **Table 2** reports singlet-triplet energy gaps for unsaturated stannylenes.

Synthetic routes to these unsaturated triplet stannylenes should be achievable. A retro-synthetic analysis containing potentially successful synthetic routes to a family of unsaturated ground-state triplet silylenes, germylenes, and stannylenes is shown in **Scheme 2**.

Retrosynthetic Analysis

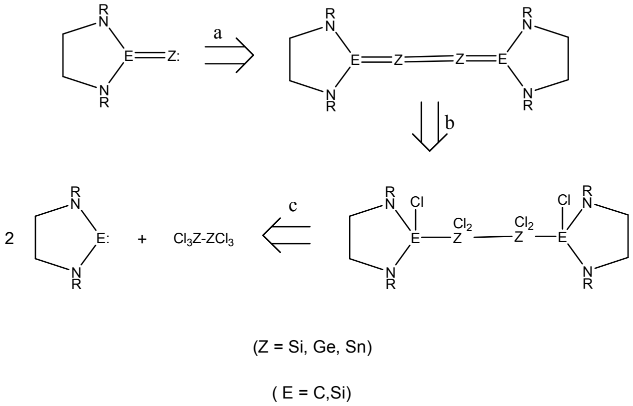

a. For thermal dissociation of disilene to two silylenes, see [29].

b. For addition of chlorine to silicon-silicon pi-bonds of disilenes, see [30].

c. For a computational study of an insertion by an N-heterocyclic silylene into a Cl–Si bond, see [31].

Scheme 2. Scheme for the retro-synthetic routes to the unsaturated ground state triplet silylenes, germylenes, and stannylenes.

5. Acknowledgments

AB and PR acknowledge the facilities at the Department of Chemistry, University of Mauritius, Réduit, Mauritius. PPG would like to thank the United States National Science Foundation for financial support of this research under NSF grant CHE-1213696. HFS would like to acknowledge generous support from NSF grant CHE-1361178. HFS thanks the Alexander von Humboldt Foundation for allowing a scientific visit to LMU Munich, in the laboratory of Professor Christian Ochsenfeld. The authors are thankful to anonymous reviewers for their useful comments to improve the manuscript.

6. References

1. O'Neil S. V.; Schaefer H. F.; Bender C. F. J. Chem. Phys., 1971, 55, 162-169.
2. Gaspar, P.P.; Hammond, G.S. "The Spin States of Carbenes", Carbene Chemistry, Wolfgang Kirmse, editor, Academic Press, Inc., N.Y., 1964, pp. 235-274.
3. Gaspar, P. P.; Hammond, G. S. “Spin States in Carbene Chemistry” in Carbenes Vol. II, R. A. Moss and M. Jones, Jr., eds., John Wiley & Sons, New York, 1975, Chap. 6, pp. 207-362.
4. Zhou, D.; Reiche, C.; Nag, M.; Soderquist, J. A.; Gaspar, P. P. Organometallics 2009, 28, 2595-2608.
5. Tokitoh, N.; Ando, W. “Silylenes (and Germylenes, Stannylenes, Plumbylenes)” in Reactive Intermediate Chemistry, R.A. Moss, M.S. Platz, M. Jones. Jr., eds., Wiley-Interscience, Hoboken, NJ, 2004, Chap. 14, pp. 651-715.
6. Neumann, W. P. Chem. Rev. 1991, 91, 311-334.
7. Gehrhus, B.; Lappert, M.F. Polyhedron 1998, 17, 999-1000.
8. Nag, M.; Gaspar, P.P. Organometallics 2009, 28, 5612-5622.
9. Worthington, S. E.; Cramer, C. J. J. Phys. Org. Chem. 1997, 10, 755-767.
10. Irikura K. K.; Goddard W. A.; Beauchamp J. L. *J. Am. Chem. Soc.*, 1992, 114, 48-51.
11. Li, B.-Y; Su, M.-D. Organometallics 2011, 30, 6189-6200.
12. Frisch, M. J. et al. Gaussian 09, Revision D.01, Gaussian, Inc., Wallingford CT, 2009.
13. Zhao, Y.; Truhlar, D. G. Theor. Chem. Acc. 2008, 120, 215-241.
14. Becke, A. D. J. Chem. Phys. 1988, 38, 3098-3100.
15. Becke, A. D. J. Chem. Phys. 1993, 98, 1372-1377.
16. Lee, C.; Yang, W.; Parr, R. G. Phys. Rev. B 1988, 37, 785-789.
17. For pseudopotentials of the Stuttgart-Dresden, see http://www.theochem.uni-stuttgart.de/pseudopotentials/index.en.html.
18. Huzinaga, S. J. Chem. Phys. 1965, 42, 1293-1302.
19. Dunning, T. H.; Hay P. J. In Modern Theoretical Chemistry, Schaefer, H. F., Ed. Plenum New York 1977, 3, 1-28.
20. Huzinaga, S. Approximate Atomic Wavefunctions II, University of Alberta: Edmonton, Alberta, 1971.
21. Lee, T. J.; Schaefer, H. F. J. Chem. Phys. 1985, 83, 1784-1794.
22. Schafer, A.; Horn, H.; Ahlrichs R. J. Chem. Phys. 1992, 97, 2571-2577.
23. NBO Version 3.1, Glendening E. D.; Reed A. E.; Carpenter J. E.; Weinhold F.

24. Weinhold, F.; Landis, C. R. “Valency and Bonding: A Natural Bond Orbital Donor-Acceptor Perspective” Cambridge University Press, 2005, pp 760.
25. Allred, A. L. J. Inorg. Nucl. Chem. 1961, 17, 215-221.
26. Bundhun A.; Ramasami P.; Schaefer H. F. J. Phys. Chem. A 2009, 113, 8080–8090.
27. Momeni, M. R.; Shakib, F. A. Organometallics 2011, 30, 5027-5032.
28. Bundhun, A.; Ramasami, P.; Gaspar, P. P.; Schaefer, H. F. Inorg. Chem. 2012, 51, 851-863.
29. Hiroyuki, S.; Norihiro, T.; Renji, O. Bull. Chem. Soc. Jpn. 1995, 68, 2471-2481.
30. Lee, V. Y.; McNeice, K.; Ito, Y.; Sekiguchi, A. Chem. Commun. 2011, 47, 3272-3274.
31. Driess, M.; Yao, S.; Brym, M.; van Wuellen, C.; Lentz, D. J. Am. Chem. Soc., 2006, 128, 9628-9629.

Table 1 Z=Sn predicted bond lengths (Å) and vibrational frequencies (cm^{-1}).

	Predicted Z=Sn bond lengths, Angstroms, employing BHLYP			
	$H_2C=Sn$:	**$H_2Si=Sn$:**	**$H_2Ge=Sn$:**	**$H_2Sn=Sn$:**
$^1A_1$	1.992	2.461	2.492	2.703
$^3A_2$	2.176	2.591	2.629	2.840
	$F_2C=Sn$:	**$F_2Si=Sn$:**	**$F_2Ge=Sn$:**	**$F_2Sn=Sn$:**
$^1A_1$	2.073	2.536	2.588	2.838
$^3A_2$	2.195	2.635	2.715	3.022
	$(NMeCH_2CH_2NMe)C=Sn$:	**$(NMeCH_2CH_2NMe)Si=Sn$:**	**$(NMeCH_2CH_2NMe)Ge=Sn$:**	**$(NMeCH_2CH_2NMe)Sn=Sn$:**
^1A	2.173	2.584	2.608	2.833
^3A	2.356	2.659	2.715	2.961
	(NMeCHCHNMe)C=Sn:	**(NMeCHCHNMe)Si=Sn:**	**(NMeCHCHNMe)Ge=Sn:**	**(NMeCHCHNMe)Sn=Sn:**
^1A	2.215	2.627	2.669	2.925
^3A	2.355	2.670	2.731	2.970
	Predicted Z=Sn stretching vibrational modes, cm^{-1}, employing BHLYP			
	$H_2C=Sn$:	**$H_2Si=Sn$:**	**$H_2Ge=Sn$:**	**$H_2Sn=Sn$:**
$^1A_1$	693	357	257	199
$^3A_2$	530	295	212	166
	$F_2C=Sn$:	**$F_2Si=Sn$:**	**$F_2Ge=Sn$:**	**$F_2Sn=Sn$:**
$^1A_1$	301	192	166	128
$^3A_2$	246	163	129	86

Table 2 Singlet-triplet gaps for stannylenes in eV (kcal mol^{-1} in parentheses).

	B3LYP		**BHLYP**		**OPBE**		**M06**	
$H_2C=Sn$:	0.91	(20.9)	0.67	(15.3)	0.92	(21.3)	1.04	(24.0)
$H_2Si=Sn$:	0.23	(5.4)	0.13	(2.9)	0.17	(3.9)	0.43	(9.8)
$H_2Ge=Sn$:	0.23	(5.2)	0.13	(3.0)	0.12	(2.7)	0.51	(11.8)
$H_2Sn=Sn$:	0.05	(1.1)	–0.04	(–0.9)	0.03	(0.6)	0.33	(7.6)
$F_2C=Sn$:	0.12	(2.9)	–0.06	(–1.4)	0.06	(1.3)	0.35	(8.1)
$F_2Si=Sn$:	–1.34	(–30.8)	–0.36	(–8.2)	–0.40	(–9.3)	–0.01	(–0.2)
$F_2Ge=Sn$:	–0.31	(–7.2)	–0.36	(–8.4)	–0.43	(–10.0)	–0.14	(–3.2)
$F_2Sn=Sn$:	–0.44	(–10.0)	–0.51	(–11.9)	–0.50	(–11.6)	–0.34	(–7.9)
$(NMeCH_2CH_2NMe)C=Sn$:	–0.40	(–9.3)	–0.52	(–11.9)	–0.54	(–12.4)	–0.04	(–1.0)
$(NMeCH_2CH_2NMe)Si=Sn$:	–0.60	(–13.8)	–0.65	(–14.9)	–0.72	(–16.6)	–0.28	(–6.4)
$(NMeCH_2CH_2NMe)Ge=Sn$:	–0.55	(–12.6)	–0.59	(–13.6)	–0.67	(–15.4)	–0.21	(–4.8)
$(NMeCH_2CH_2NMe)Sn=Sn$:	–0.60	(–13.8)	–0.66	(–15.2)	–0.65	(–15.1)	–0.26	(–5.9)
(NMeCHCHNMe)C=Sn:	–0.56	(–12.9)	–0.67	(–15.5)	–0.70	(–16.2)	–0.22	(–5.0)
(NMeCHCHNMe)Si=Sn:	–0.68	(–15.6)	–0.81	(–18.8)	–0.94	(–21.7)	–0.46	(–10.7)
(NMeCHCHNMe)Ge=Sn:	–0.80	(–18.6)	–0.82	(–18.9)	–0.94	(–21.7)	–0.46	(–10.7)
(NMeCHCHNMe)Sn=Sn:	–0.89	(–20.4)	–0.92	(–21.1)	–1.00	(–23.1)	–0.54	(–12.5)

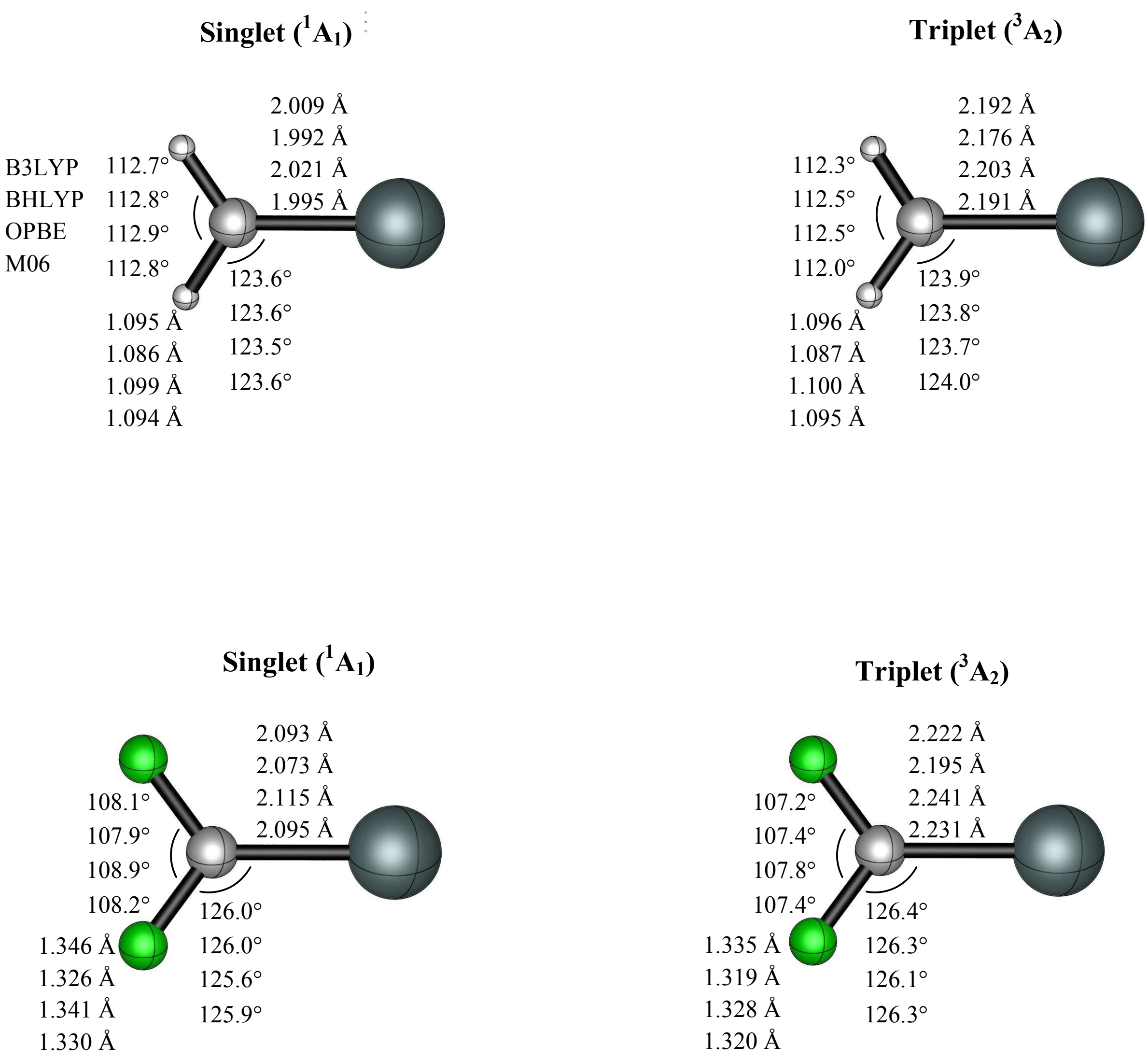

Figure 1. Equilibrium geometries for the lowest lying singlet and triplet states of $H_2C=Sn:$ and $F_2C=Sn:$.

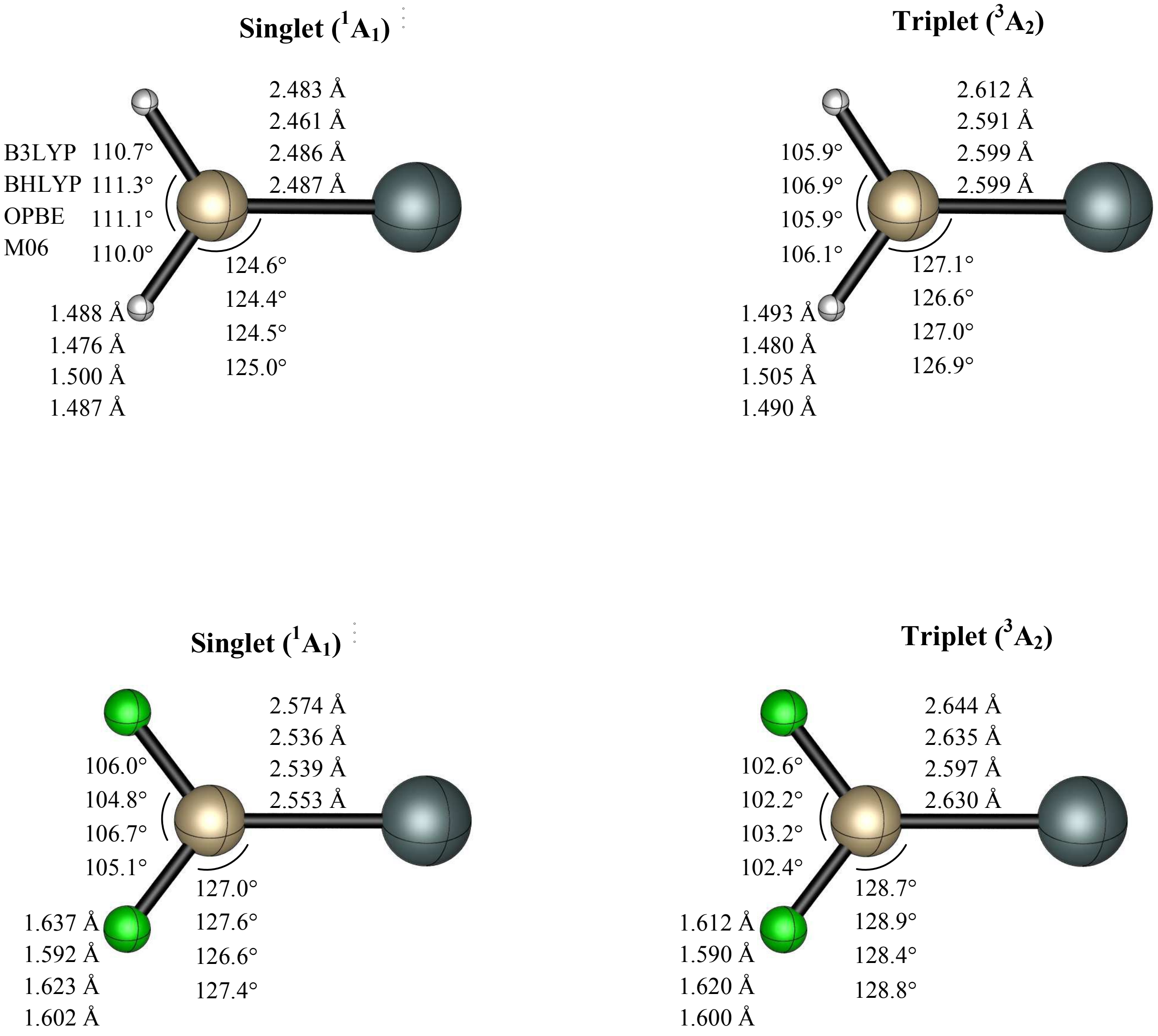
Singlet ($^1A_1$)
Triplet ($^3A_2$)
Singlet ($^1A_1$)
Triplet ($^3A_2$)

Figure 2. Equilibrium geometries for the lowest lying singlet and triplet electronic states of $H_2Si{=}Sn$: and $F_2Si{=}Sn$:.

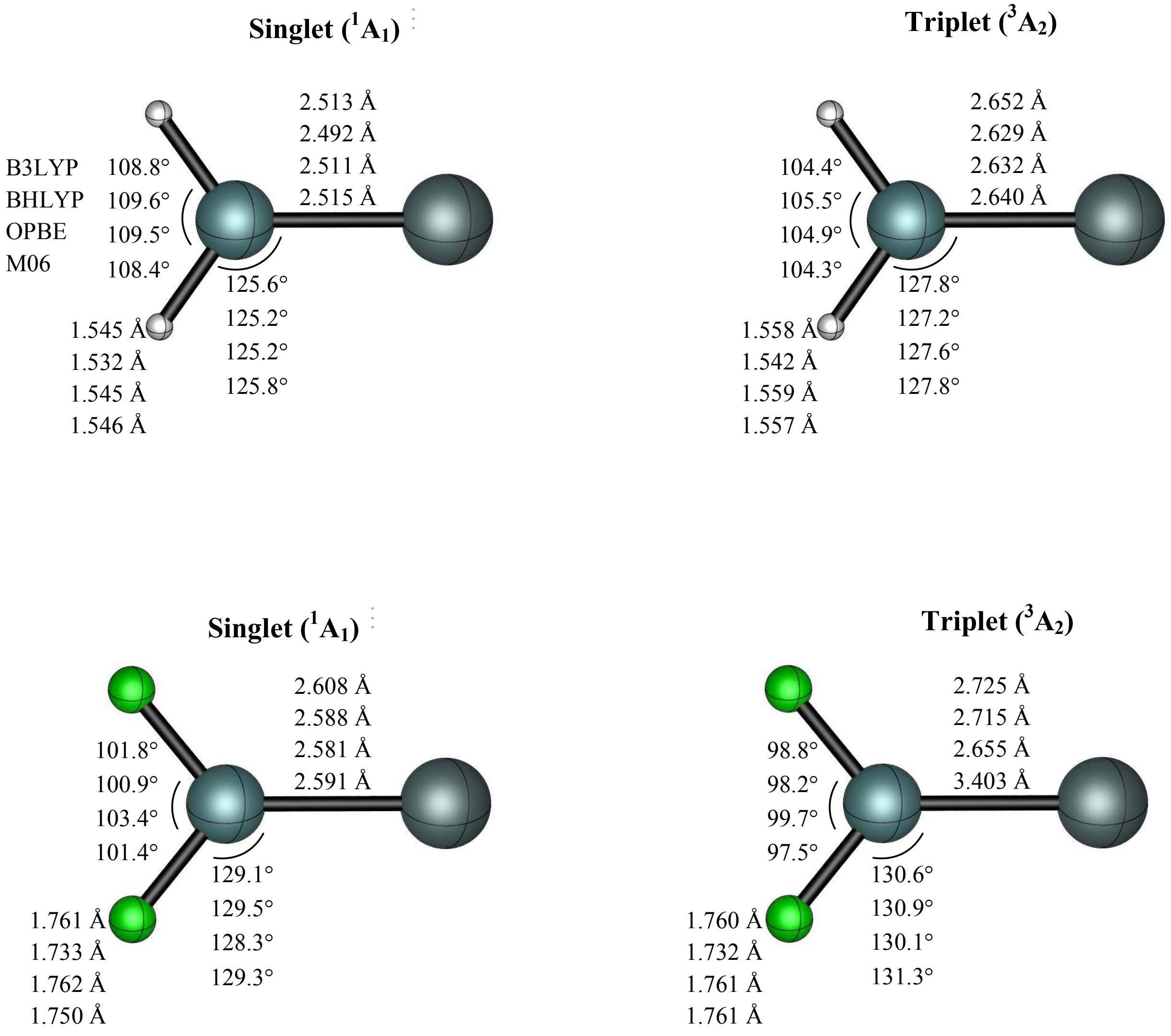

Figure 3. Equilibrium geometries for the lowest lying singlet and triplet states of H_2Ge=Sn: and F_2Ge=Sn:.

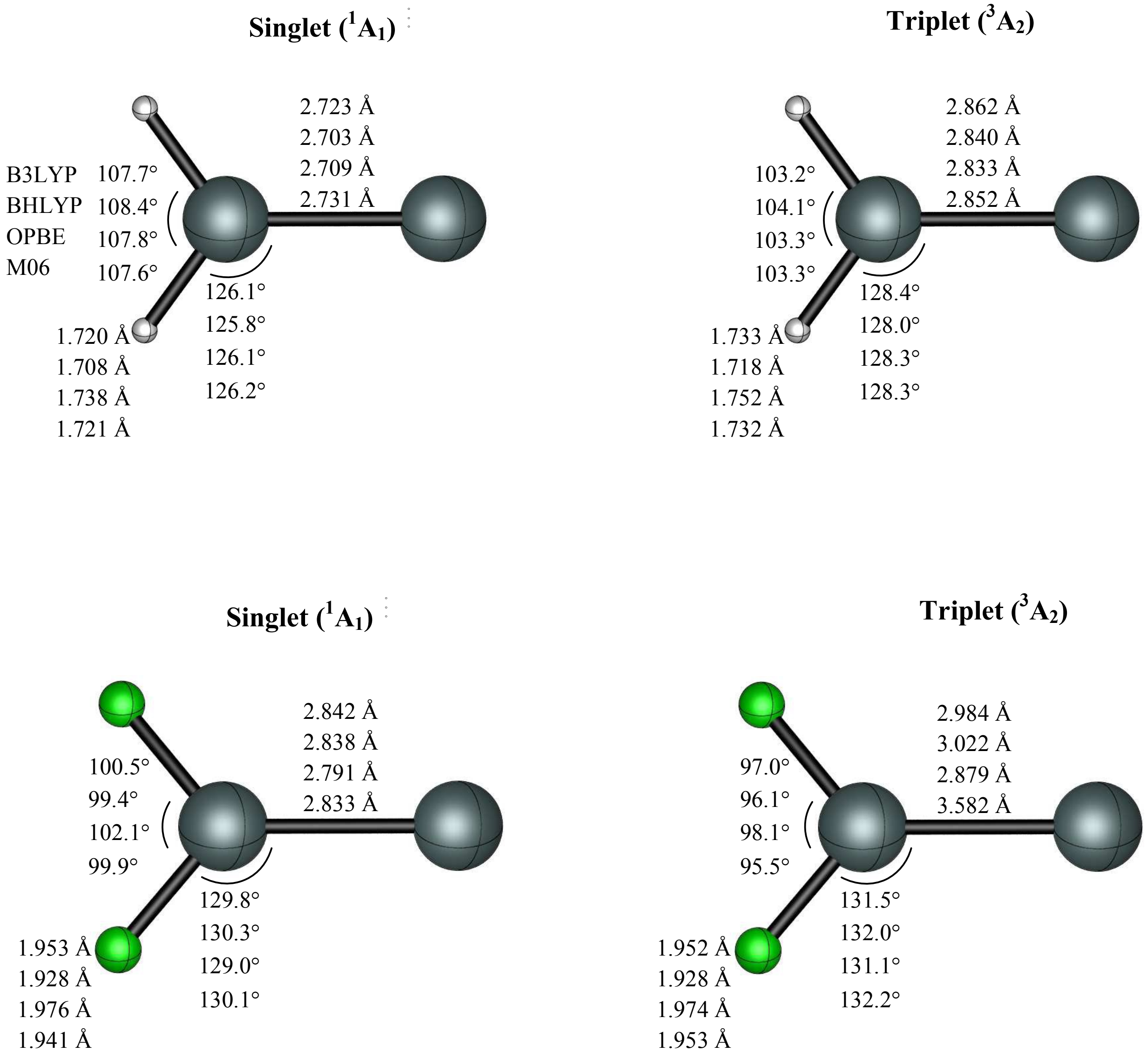

Singlet ($^1A_1$)

Triplet ($^3A_2$)

Singlet ($^1A_1$)

Triplet ($^3A_2$)

Figure 4. Equilibrium geometries for the lowest lying singlet and triplet states of $H_2Sn{=}Sn$: and $F_2Sn{=}Sn$:.

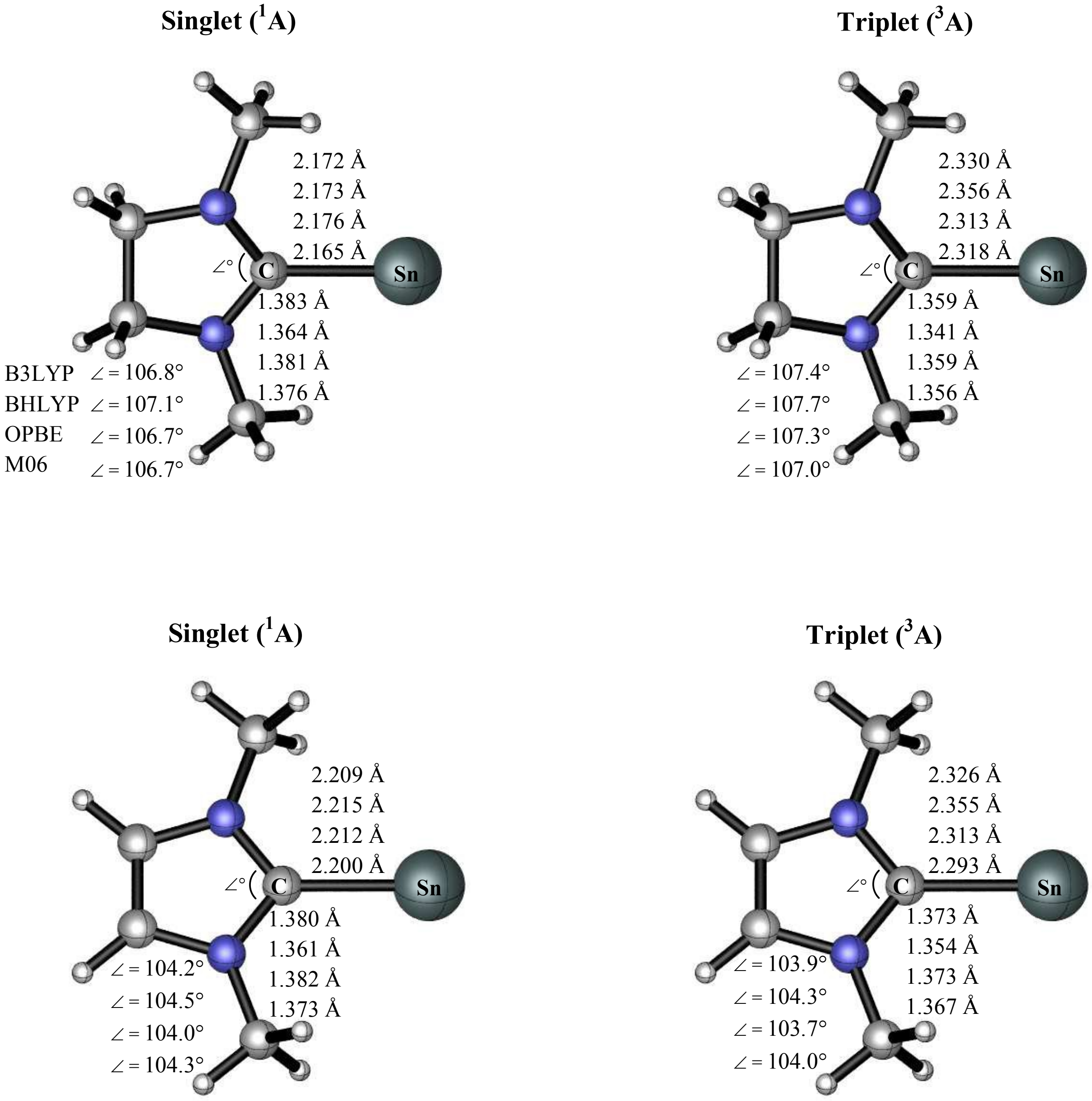

Figure 5. Equilibrium geometries for the lowest lying singlet and triplet states of $(NMeCH_2CH_2NMe)C{=}Sn$: and $(NMeCHCHNMe)C{=}Sn$:.

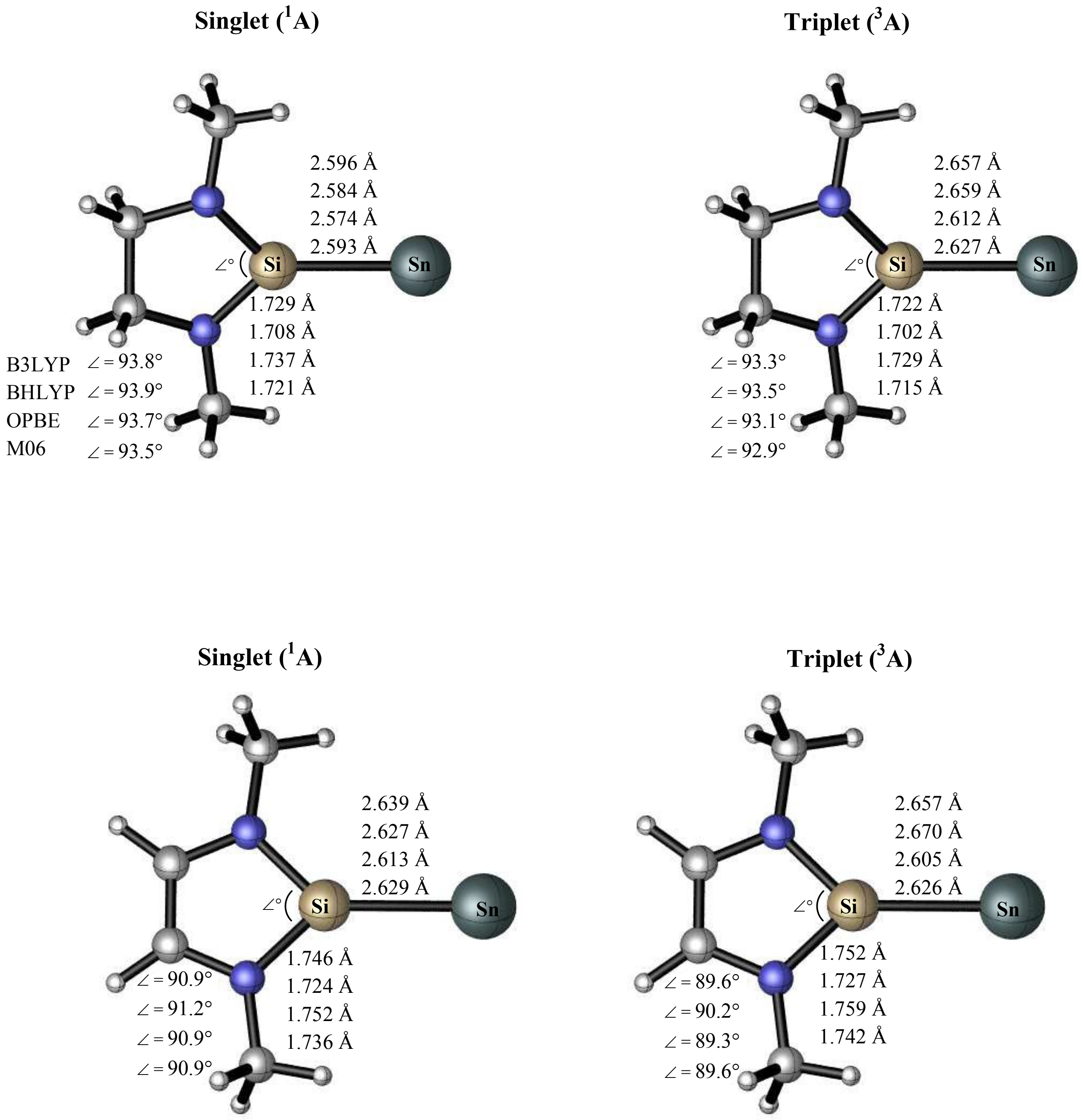

Figure 6. Equilibrium geometries for the lowest lying singlet and triplet states of (NMeCH$_2$CH$_2$NMe)Si=Sn: and (NMeCHCHNMe)Si=Sn:.

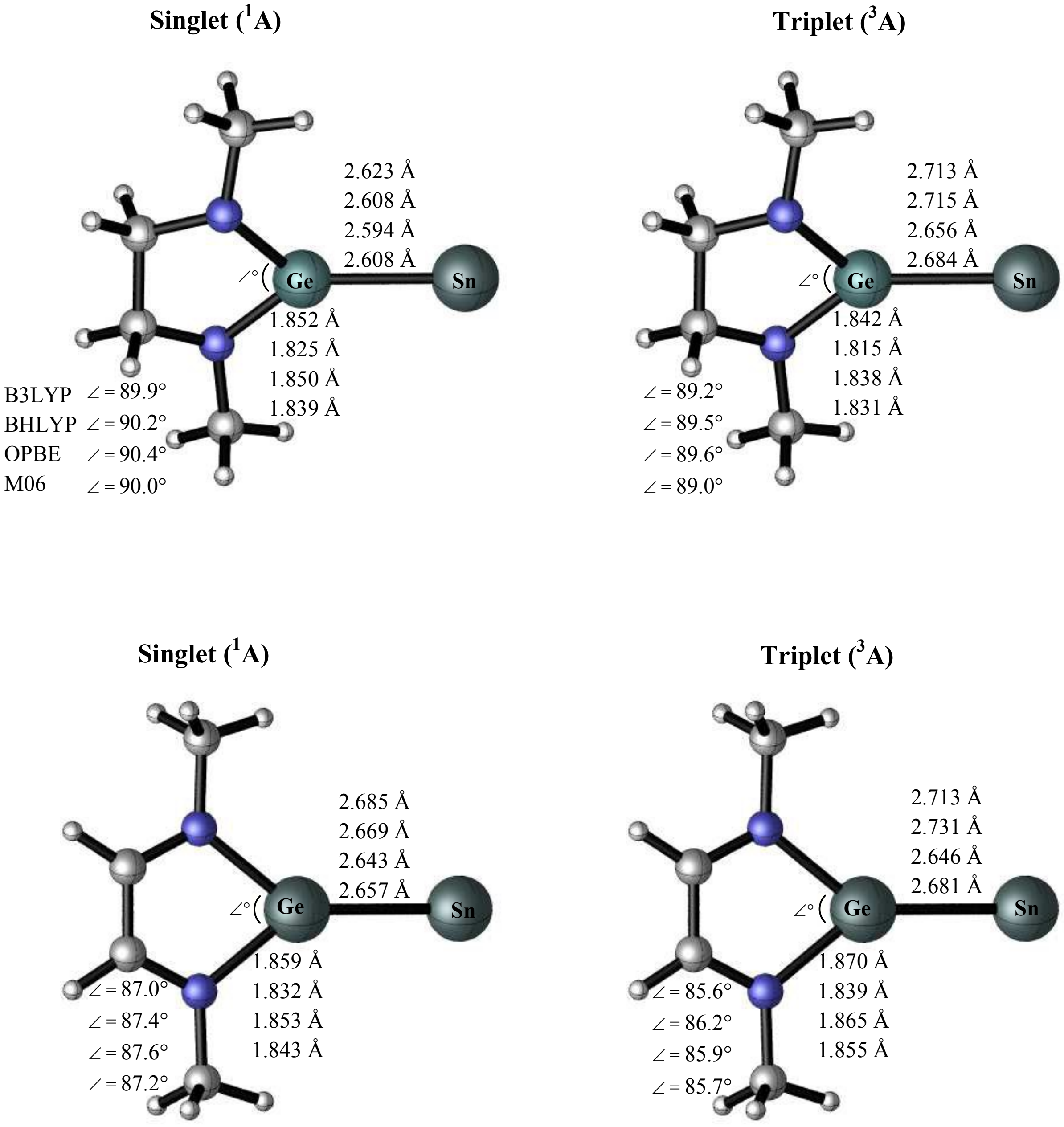

Figure 7. Equilibrium geometries for the lowest lying singlet and triplet states of (NMeCH$_2$CH$_2$NMe)Ge=Sn: and (NMeCHCHNMe)Ge=Sn:.

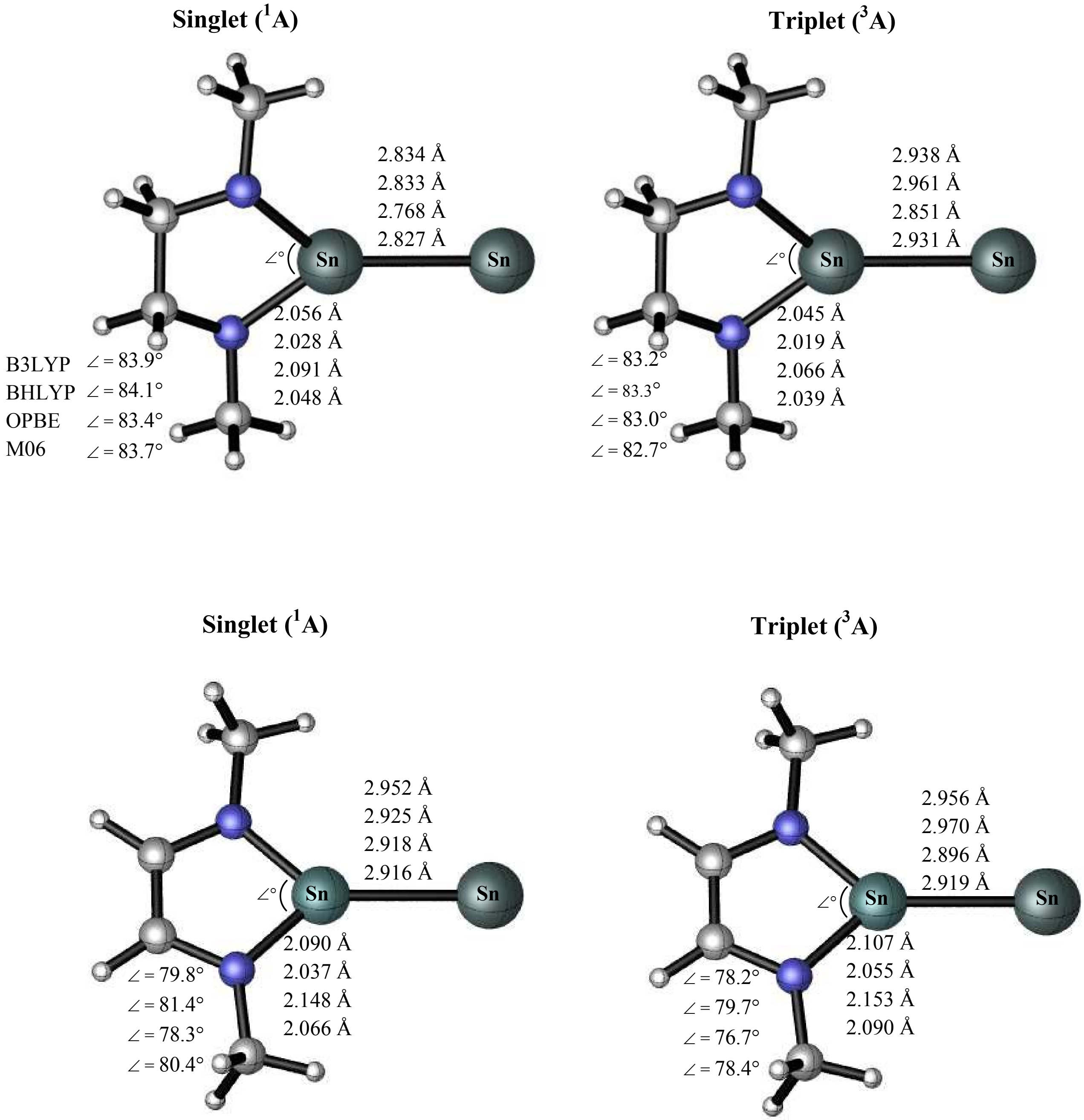

Figure 8. Equilibrium geometries for the lowest lying singlet and triplet states of (NMeCH_2CH_2NMe)Sn=Sn: and (NMeCHCHNMe)Sn=Sn:.

Graphical Abstract

Unsaturated Stannylenes

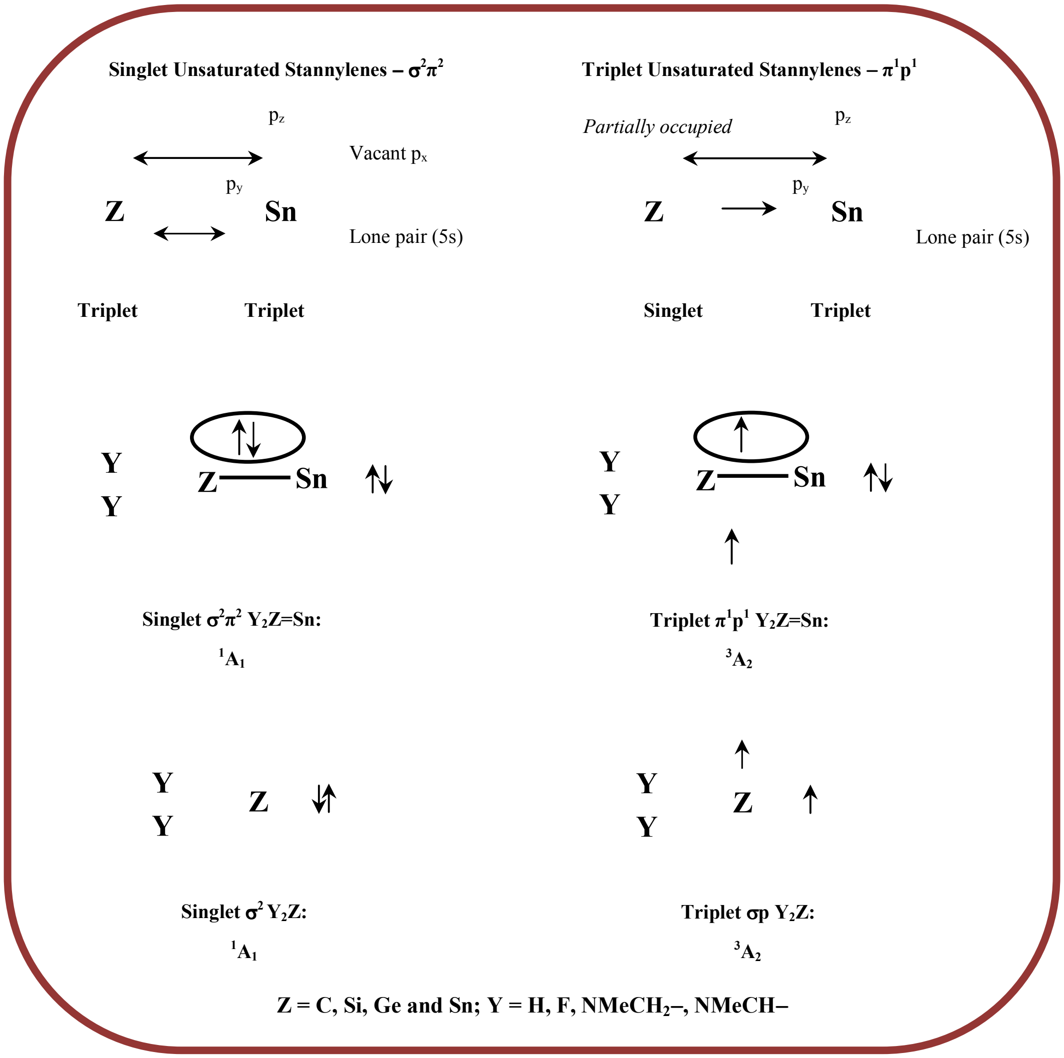

Scheme 1. Distribution of electrons between the Y_2Z: moiety and the triplet Sn atom in Y_2Z=Sn: and representations of singlet and triplet Y_2Z=Sn: and Y_2Z: electronic configurations.